

Lattice Dynamics and Baric Behavior of Phonons in the Hg_2Br_2 Model Ferroelastics

E. M. Roginskii^{a,*}, A. S. Krylov^b, and Yu. F. Markov^a

^a Ioffe Institute, St. Petersburg, 194021 Russia

^b Kirensky Institute of Physics, Krasnoyarsk Scientific Center, Siberian Branch,
Russian Academy of Sciences, Krasnoyarsk, 660036 Russia

*e-mail: e.roginskii@mail.ioffe.ru

Received July 18, 2018

Abstract—Raman spectra of Hg_2Br_2 model improper ferroelastic crystals have been investigated in a wide range of high hydrostatic pressures. Baric dependences of the phonon frequencies have been obtained; of greatest interest are the observed soft mode originating from the slowest TA_1 acoustic branch at the Brillouin zone boundary (X point) of the tetragonal phase and the anomalous behavior of this mode. In the ferroelastic phase spectra, the ignition of the second acoustic TA_2 from the same point has also been detected and its baric behavior has been studied. Under sufficiently high pressures, splitting of doubly degenerate phonons with the E_g symmetry has been observed and explained. The parameters of the Grüneisen constants have been determined from the baric dependences of the phonon frequencies and discussed.

DOI: 10.1134/S1063783419020227

1. INTRODUCTION

The Hg_2Hal_2 (Hal = F, Cl, Br, or I) mercurous halide crystals have a very simple room-temperature structure consisting of linear molecule chains Hal–Hg–Hg–Hal parallel to the $C_4(Z)$ optical axis, which are weakly bound with each other and form a body-centered tetragonal D_{4h}^{17} lattice with two molecules in the unit cell (Fig. 1) [1]. The chain structure of these crystals causes a very strong anisotropy of their physical properties, including elastic and optical ones. These crystals exhibit the unique physical characteristics; in particular, among solids, they have the record low transverse (TA) speeds of sound $V_{[110]}^{[110]} = 282$ m/s (Hg_2Br_2) and 253 m/s (Hg_2I_2), the record high birefringence $\Delta n = +0.85$ (Hg_2Br_2) and $+1.48$ (Hg_2I_2), and acoustooptical interaction for the TA wave $M_2 = 1804 \times 10^{-18}$ CGS units (Hg_2Br_2) and 4284×10^{-18} CGS units (Hg_2I_2) [2].

These unique properties make it possible to successfully use the discussed crystals in engineering as basic elements of polarizers, acoustic delay lines, acoustooptical filters, modulators, deflectors, etc.

In addition, isomorphous crystals of this family evoke considerable interest as model crystal systems for solving general problems of the structural phase transitions (PTs). Upon cooling to $T_c = 186$ K (Hg_2Cl_2) and $T_c = 144$ K (Hg_2Br_2), these crystals

undergo the improper ferroelastic PTs $D_{4h}^{17} \rightarrow D_{2h}^{17}$ from the tetragonal to orthorhombic phase. The PTs are induced by condensation of the slowest and lowest-frequency TA branch at the X point of the Brillouin zone (BZ) of the tetragonal paraphase and accompanied by the unit cell doubling at $T \leq T_c$, $T \rightarrow \Gamma$ folding in the BZ, and the occurrence of spontaneous deformation and ferroelastic domains [3–5].

However, in the isomorphous Hg_2I_2 crystals, the PT does not occur under atmospheric pressure even at very low (down to 1.5 K) temperatures, but in the Raman spectra, softening of one of the low-intensity low-frequency vibrations was observed [6]. Analogously to the effects in the isomorphous Hg_2Cl_2 and Hg_2Br_2 crystals, this vibration was assumed to be an overtone of the soft TA branch from the BZ boundary (X point). Under atmospheric pressure, the Hg_2I_2 crystals are virtual ferroelastics ($T_c \approx -20$ K). The PTs in these crystals were only implemented under the hydrostatic pressure (9 kbar) at $T = 300$ K [7]. Close attention was paid to examination of the baric behavior of soft modes, both in the paraphase ($P < P_c$) and in the ferroelastic phase ($P > P_c$) [8, 9].

Recently, we have theoretically and experimentally investigated the isomorphous and model Hg_2Cl_2 ferroelastic [10] and found the baric behavior of phonons, including soft ones, and a fundamental effect, specifically, a new structural PT.

In this study, we continue these baric investigations, but already on different, also model and isomorphic Hg_2Br_2 crystals.

2. EXPERIMENTAL

The high (up to 13 GPa) hydrostatic pressure experiments were conducted on a setup with diamond anvils at a temperature of 295 K. The diameter of a chamber with the sample was 0.25 mm and its height was 0.1 mm. Under pressures of up to 4–5 GPa, different oils were used as pressure transmitting media and, at the higher pressures, a thoroughly dehydrated mixture of ethyl and methyl alcohols was used. The pressure in the diamond chamber was determined from the shift of the luminescence band of rubine, the microcrystal of which was placed near the sample under study [11]. The pressure measurement error was no larger than 0.05 GPa.

In studying the Raman spectra, the polarized 514.5 nm radiation of an Ar laser (Spectra-Physics Stabilite 2017) with a power of 100 mW (20 mW on the sample) was used as an excitation source. The spectra in the 180° geometry were recorded using a Horiba Jobin Yvon T64000 spectrometer in the frequency range of 20–400 cm^{-1} .

The previously studied Hg_2Br_2 crystals were split along the $\{110\}$ and $\{1\bar{1}0\}$ cleavage planes and single crystals of a required size were selected from a set of cleaved samples for performing the measurements. The samples no more than about $0.2 \times 0.2 \times 0.2$ mm in size were placed in a chamber with diamond anvils for optical investigations, including polarization ones, under pressures from 0.2 to 13 GPa.

3. RESULTS AND DISCUSSION

Since the unit cell of the tetragonal Hg_2Br_2 crystals (sp. gr. D_{4h}^{17}) consists of the only linear molecule (four atoms), then, according to the group theory, the decomposition of the vibrational spectrum by the irreducible representations (IRs) has the form

$$\Gamma = 2A_{1g} + 2A_{2u} + 2E_u + 2E_g.$$

In this case, only two vibrations of the A_{1g} symmetry and two vibrations of the E_g symmetry will be active in the Raman spectra. The eigenvectors (normal coordinates) of these vibrations are shown in Fig. 1. The low-frequency vibrations denoted by ν_1 and ν_2 in Fig. 1 have the E_g symmetry and will therefore be active in the Raman spectra in the $XZ(YZ)$ polarizations; the fully symmetric vibrations A_{1g} (ν_3 and ν_4) are resolved in the Raman spectra in the XX , YY , and ZZ polarizations.

It should be noted that the first doubly degenerate vibration of the E_g symmetry is libration, i.e., the libration of a linear molecule as an integer with respect to

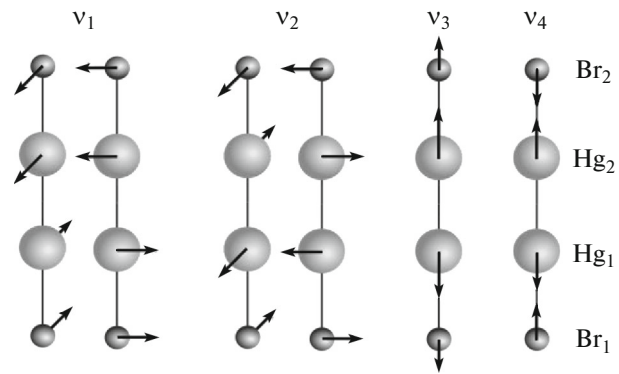


Fig. 1. Normal vibration vectors of the D_{4h}^{17} (Hg_2Br_2) tetragonal lattice.

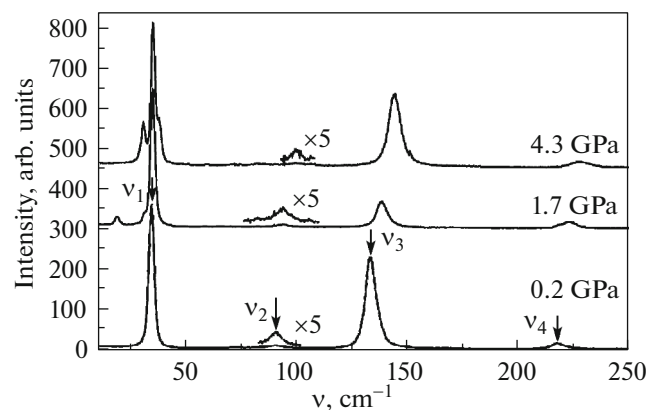


Fig. 2. Raman scattering spectra of the Hg_2Br_2 crystals under the low (0.2 GPa) and high (1.7 and 4.3 GPa) hydrostatic pressures.

the horizontal X (or Y) axis denoted by ν_1 ; the second vibration of the E_g symmetry is deformation zigzag (ν_2); the fully symmetric valence vibrations A_{1g} correspond mainly to the Hg–Hg (ν_3) and Br–Hg (ν_4) displacements (see Fig. 1).

Figure 2 shows the spectra of the Hg_2Br_2 crystals under different hydrostatic pressures (0.2, 1.7, and 4.3 GPa). In all the spectra in Fig. 2, one can see two lines corresponding to the E_g symmetry vibrations and two lines corresponding to the A_{1g} symmetry, which is consistent with the results of group-theoretical analysis. However, the spectra of the samples under pressure above 0.2 GPa contain the singularities related to the structural phase transition $D_{4h}^{17} \rightarrow D_{2h}^{17}$; in particular, significant comparable ν_2 , ν_3 , and ν_4 frequency shifts are observed, which are caused by the unit cell doubling and, in the region of the librational vibration ν_1 , convincingly manifest themselves as minor phonon frequency shifts and anomalous behavior, including

splitting of the degenerate vibrations $\nu_1(E_g)$ (Figs. 2 and 3).

Recall that the phase transition $D_{4h}^{17} \rightarrow D_{2h}^{17}$ is induced by the condensation of the transverse TA_1 phonon at the BZ boundary (X point), the IR of which is X_3^- . Table 1 gives the correspondence between the IRs of phonons of the tetragonal (D_{4h}^{17}) and orthorhombic (D_{2h}^{17}) phases, which was obtained from the results of group-theoretical analysis performed using the Bilbao Crystallographic Server (BCS) server software [12]. In Table 1, one can see, in particular, that the phase transition eliminates the degeneracy of the transverse acoustic and optical phonons ν_1 and ν_5 . According to the data given in Table 1, the IR E_g of the tetragonal phase is divided in two IRs $B_{1g} + B_{2g}$ and the IR E_u of the tetragonal phase is divided into two IRs $B_{1u} + B_{2u}$. In addition, as a result of the throw $X \rightarrow \Gamma$, new phonons arise at the center of the BZ of the orthorhombic phase, the IRs of which are $A_u, B_{2u}, B_{3u}, A_g, B_{1g},$ and B_{3g} , which leads to the occurrence of new lines in the Raman spectra. A striking example of such enrichment of the spectrum is the phonon with the A_g symmetry of the orthorhombic phase, which is genetically related to the transverse TA_2 acoustic vibration of the tetragonal phase (soft mode) and the phonon with the B_{3g} symmetry genetically related to the second transverse acoustic phonon at the BZ boundary of the tetragonal phase.

To illustrate the effects of the phase transition in these crystals, Fig. 3 presents the Raman spectra obtained under different hydrostatic pressures in the low-frequency range (0–50 cm^{-1}). The most interesting fact established when studying the lattice dynamics of the Hg_2Br_2 crystals under high hydrostatic pressures was a significant strengthening of the lowest-frequency A_g phonon denoted by $\nu_{\text{sm}}(TA_1)$ in Fig. 3, the genesis of which was discussed above, with increasing pressure.

In addition, note the occurrence of a Raman phonon with the B_{1g} symmetry in the spectrum on the low-frequency wing of the line related to the librational vibration ν_1 (see Figs. 2 and 3). The occurrence of this maximum was also discussed above and the pressure dependence of the frequency of this phonon can be described as a slight softening.

In the Raman spectra, we could find maxima related to the two-phonon interaction and IR-active phonons, as, for example, in the case of Hg_2I_2 crystals [7, 8]. However, this is fairly difficult, since the experiments in a diamond chamber with small crystals and a small chamber aperture lower manifold the useful signal. In addition, we cannot ignore the effect of the polydomain form of the investigated samples and a significant shift of the absorption edge to the low-fre-

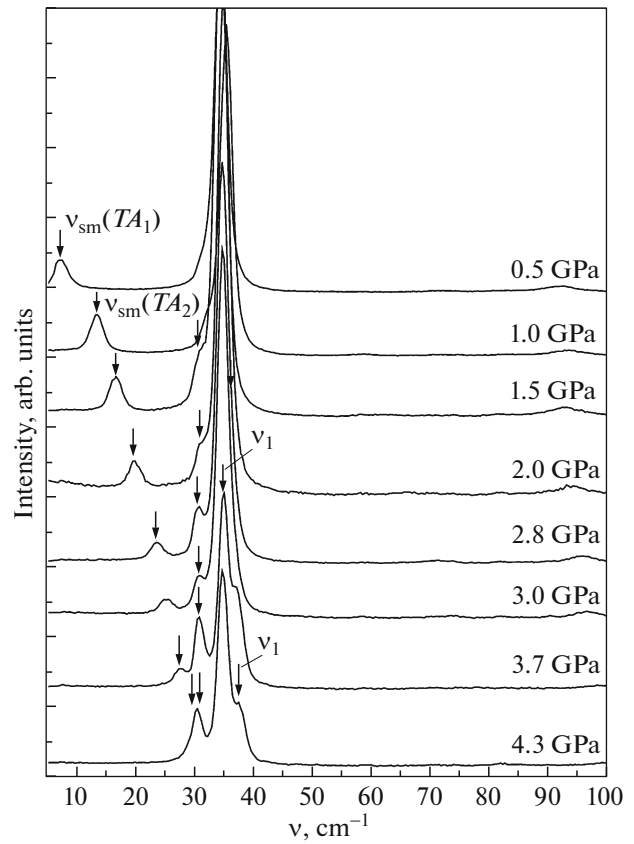


Fig. 3. Low-frequency Raman scattering spectra of the Hg_2Br_2 crystals under different hydrostatic pressures.

quency spectral region, which degrades the sample transparency with increasing pressure in the chamber.

Under pressures above 3 GPa, the spectra demonstrate splitting of the doubly degenerate vibration ν_1

Table 1

Mode	D_{4h}^{17}, Γ	D_{4h}^{17}, X	D_{2h}^{17}, Γ
ν_1	E_g	X_3^+	$B_{1g} + B_{2g}$
		X_4^+	A_u
$\nu_{3,4}$	A_{1g}	X_1^+	B_{3u}
		X_1^+	A_g
$\nu_5 + TA_1 + LA$	E_u	X_1^+	B_{2u}
		X_3^-	$B_{1u} + B_{2u}$
$\nu_6 + TA_2$	A_{2u}	X_4^-	A_g
		X_2^-	B_{3g}
			B_{3u}
			B_{1g}

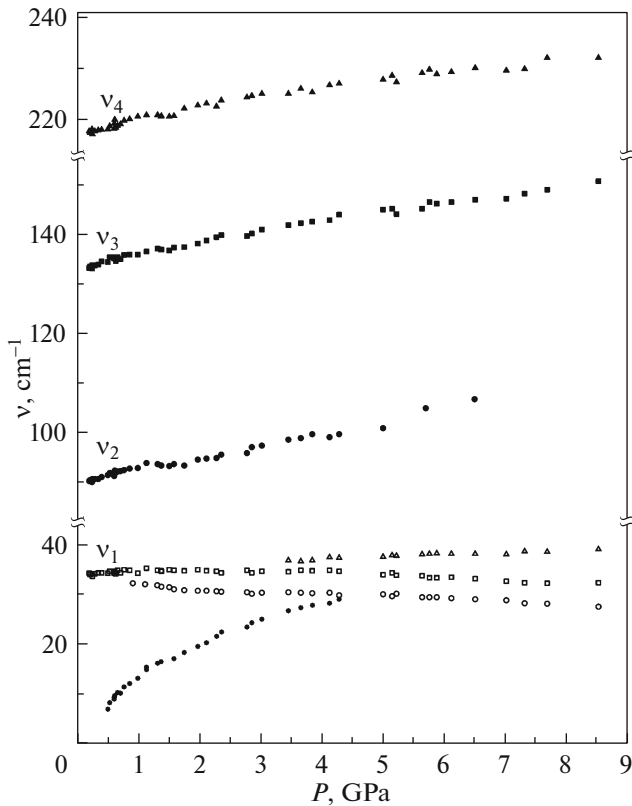


Fig. 4. Baric dependences of the phonon frequencies in the Hg_2Br_2 crystals. Asterisks show the $\nu_{\text{sm}}(TA_1)$ mode frequency; open circles, the $\nu_{\text{sm}}(TA_2)$ mode frequency; open squares and triangles, the librational vibration ν_1 ; closed circles, the deformation vibration ν_2 ; and closed squares and triangles, valence vibrations ν_3 and ν_4 , respectively.

into two components (the lines corresponding to the phonons of the B_{1g} and B_{2g} symmetries, see Table 1) related to the structural phase transition and loss of the fourth-order axis.

Figure 4 shows the dependences of the fundamental vibration frequencies in the Hg_2Br_2 crystals on the applied hydrostatic pressures, which can be described with good accuracy by the linear approximation and thereby determine the frequency variation dynamics for each phonon active in the Raman spectra. In particular, the rate of change of the vibration $\nu_{\text{sm}}(TA_1)$ was found to be $-0.38 \text{ cm}^{-1}/\text{GPa}$; for the librational vibrations ν_1' and ν_1'' , the rates were -0.2 and $0.4 \text{ cm}^{-1}/\text{GPa}$, respectively; for the deformation vibration ν_2 , it was $2.0 \text{ cm}^{-1}/\text{GPa}$; and, finally, for the valence vibrations ν_3 and ν_4 , the rates were 2.05 and $1.87 \text{ cm}^{-1}/\text{GPa}$, respectively.

It is worth noting that the phonon frequencies ν_1 are almost pressure-independent; i.e., the Gruneisen constants characterizing the baric behavior are very small and even negative. Similar effects were observed

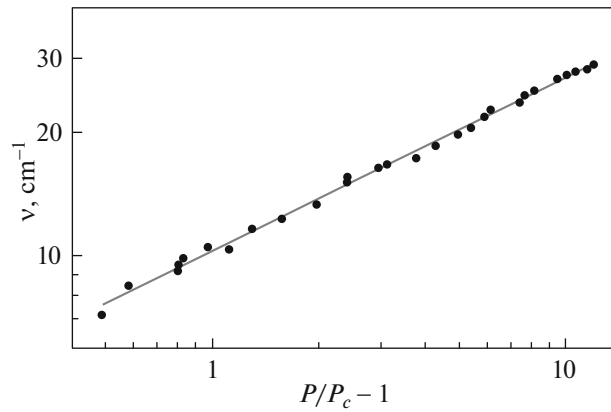


Fig. 5. Baric behavior of the soft mode in the Hg_2Br_2 crystals in the double logarithmic scale and as a function of the reduced pressure $\nu_{\text{sm}}(p)$, where $p = P/P_c - 1$.

for the Hg_2I_2 crystals [9]. Such an anomalous behavior can be attributed to the character of this vibration. As was shown in [13], the Hg_2Hal_2 crystals are quasi-molecular compounds; therefore, in addition to the Coulomb interaction, the long-range interaction (e.g., van der Waals forces) works in these crystals. The strongest Coulomb interaction exists between molecules located in the nodes and the bulk of the unit cell, since they are closest to each other. Moreover, the Coulomb interaction exists mainly between the nearest halves of molecules in the nodes and the bulk ($\text{Hg}-\text{Br}$). In the case of a librational vibration, these halves of the nearest molecules maximally approach each other in phase and move from each other in antiphase; in this case, the competing cation–anion attraction and cation–cation (anion–anion) repulsion of the neighboring halves of molecules arise. As a result, this interaction is compensated and the pressure-induced approaching of molecules does not significantly affect the force constant variation and even leads to their decrease and, consequently, reduction of the frequency of this vibration.

The dynamics of the vibrations ν_2 , ν_3 , and ν_4 is absolutely different: they exhibit strong frequency shifts with increasing hydrostatic pressure (see Fig. 2) and, consequently, large positive Gruneisen constants. These large frequency shifts can be attributed to the strong effect of the applied hydrostatic pressure on the ion-covalent bonds inside molecules, which lead to the anomalous growth of intramolecular force constants ($\nu \sim \sqrt{k/\mu}$).

Figure 5 shows the baric dependence of the phonon frequency ν_{extcm} , which can be described by the formula $\nu_{\text{sm}} \sim [(P - P_c)/P_c]^\beta$, where $[(P - P_c)/P_c] = p$ is the reduced pressure and the PT pressure at room temperature is $P_c = 0.3 \text{ GPa}$. To determine strictly the critical index β , which characterizes the model of the phase transition that occurred at 0.3 GPa , this relation

was built in the double logarithmic scale and was found to be linear (Fig. 5); the slope of the curve gives directly the critical index $\beta = 0.4 \pm 0.02$.

In principle, the obtained value does not contradict the model of the phase transition occurring near the tricritical point determined earlier from the temperature dependence of the analogous soft mode observed in [3–5].

4. CONCLUSIONS

Thus, we studied the Raman spectra of the Hg_2Br_2 crystals under high hydrostatic pressures and observed the ignition in the Raman phonon spectra, including soft ones, interpreted and discussed the results obtained, and confirmed the model of the phase transition $D_{4h}^{17} \rightarrow D_{2h}^{17}$ induced by a decrease in the temperature of Hg_2Br_2 [3–5].

ACKNOWLEDGMENTS

This study was supported by the Presidium of the Russian Academy of Sciences, Programs no. 1.4 “Urgent Problems of Low-Temperature Physics” and no. 1.7 “Physics of Condensed Matter and New-Generation Materials.”

The authors are grateful to Yu.E. Kitaev for fruitful discussions.

REFERENCES

1. H. Mark and J. Steinbach, *Z. Kristallogr.* **64**, 78 (1926).

2. *Proceedings of the 2nd International Symposium on Univalent Mercury Halides, ŠFR, Trutnov, 1989.*
3. Ch. Barta, A. A. Kaplyanskii, V. V. Kulakov, B. Z. Mal'kin, and Yu. F. Markov, *Sov. Phys. JETP* **43**, 218 (1976).
4. A. A. Kaplyanskii, Yu. F. Markov, and Ch. Barta, *Izv. Akad. Nauk SSSR, Ser. Fiz.* **43**, 1641 (1979).
5. B. S. Zadokhin, Yu. F. Markov, and A. S. Yurkov, *J. Exp. Theor. Phys.* **77**, 286 (1993).
6. Ch. Barta, A. A. Kaplyanskii, Yu. F. Markov, and V. Yu. Mirovitskii, *Sov. Phys. Solid State* **27**, 1497 (1985).
7. Yu. F. Markov and A. Sh. Turaev, *JETP Lett.* **63**, 241 (1996).
8. Yu. F. Markov, V. Yu. Mirovitskii, and E. M. Roginskii, *Tech. Phys. Lett.* **40**, 992 (2014).
9. Yu. F. Markov, V. Yu. Mirovitskii, and E. M. Roginskii, *Phys. Solid State* **57**, 480 (2015).
10. E. M. Roginskii, A. S. Krylov, Yu. F. Markov, and M. B. Smirnov, *Bull. Russ. Acad. Sci.: Phys.* **80**, 1033 (2016).
11. F. Datchi, A. Dewaele, P. Loubeyre, R. Letoullec, Y. le Godec, and B. Canny, *High Press. Res.* **27**, 447 (2007).
12. M. I. Aroyo, A. Kirov, C. Capillas, J. M. Perez-Mato, and H. Wondratschek, *Acta Crystallogr. A* **62**, 115 (2006). www.cryst.ehu.es.
13. E. M. Roginskii, Yu. F. Markov, and M. B. Smirnov, *Phys. Solid State* **57**, 467 (2015).

Translated by E. Bondareva